International Journal of GEOMATE, March, 2025 Vol.28, Issue 127, pp.96-103
ISSN: 2186-2982 (P), 2186-2990 (O), Japan, DOI: https://doi.org/10.21660/2025.127.g14132
Geotechnique, Construction Materials and Environment

EXPERIMENTAL STUDY ON THE AIR PERMEABILITY CHARACTERISTICS OF NONWOVEN MEDIA IN BAGHOUSE FILTERS

Kittipos Loksupapaiboon[1,5], Angtida Punyaponchai[2,5], Juthanee Phromjan[3,5], Panit Kamma[4,5] and *Chakrit Suvanjumrat[2,5]

[1]Department of Maritime Engineering, Faculty of International Maritime Studies, Kasetsart University Sriracha Campus, Thailand
[2]Department of Mechanical Engineering, Faculty of Engineering, Mahidol University, Thailand
[3]Department of Mechanical Engineering, Faculty of Engineering, King Mongkut's University of Technology Thonburi, Thailand
[4]Department of Mechanical and Manufacturing Engineering, Faculty of Science and Engineering, Kasetsart University, Chalermphrakiat Sakon Nakhon Province Campus, Thailand
[5]Laboratory of Computer Mechanics for Design (LCMD), Faculty of Engineering, Mahidol University, Thailand

*Corresponding Author, Received: 14 Dec. 2024, Revised: 28 Jan. 2025, Accepted: 30 Jan. 2025

ABSTRACT: This study aimed to design and evaluate a dust collector capable of capturing particles smaller than 10 microns, addressing the critical challenge of reducing air pollution caused by industrial exhaust gases. Dust particles emitted from various industrial plants significantly contribute to air pollution and pose severe health risks. Filtration using nonwoven filter media has emerged as an effective technology for environmental protection. A series of experiments was conducted to evaluate the efficiency of nonwoven filters under varying operating conditions. The tests utilized filter materials with different air permeability properties in a pilot-scale dust collector. Measurements of filtration pressure drop and gas velocity revealed that the pressure drop increased with higher gas velocity but decreased with increased filter media permeability. The pressure drop was characterized by a second-order polynomial equation of filtration velocity, further linked to the Darcy-Forchheimer equation for porous media. The results demonstrated two distinct patterns of pressure drop increase influenced by air permeability. Filters with lower air permeability exhibited comparable pressure drop trends. The experimental data showed strong agreement with the modeled pressure drop values, achieving a coefficient of determination (R^2) exceeding 0.989. This high level of accuracy underscores the effectiveness of the model for designing air filtration systems.

Keywords: Air permeability, Dust collector, Filter, Nonwoven media, Pressure drop.

1. INTRODUCTION

Air pollution is widely recognized as a significant environmental issue, with adverse effects on human health resulting from the deterioration of air quality. This decline is associated with various activities, including industrial operations, transportation, forest fires, and the combustion of fuels [1]. Air quality standards for ambient air take particle size into account by measuring fine particulate matter, such as PM2.5 and PM10. These airborne particles, particularly fine particles, have attracted increasing attention as pollutants due to their ability to be easily transported over long distances. The growing concern over air pollution and the need to protect human health, combined with recent industrial expansion, underscores the importance of developing effective gas purification technologies and equipment.

In industrial plants, dust particles are commonly present in exhaust gases. The separation of airborne particulates can enhance the value of by-products released into the atmosphere, thereby increasing overall industry profits. To reduce the emission of fine particles from flue gas, baghouses are widely employed to collect particulate matter from industries such as milk processing, woodwork, fly ash handling, and limestone production [2, 3]. A baghouse filter is an air pollution control device that removes particulate matter from air or gas streams using fabric filter bags housed in a casing. Key components include filter bags, cages for support, plenums for airflow direction, and mechanisms like pulse jet or shaker systems for cleaning, with efficiency measured by parameters such as differential pressure and filtration velocity. The cylindrical cartridge filter is the most prevalent type of bag used in baghouse systems. A variety of filter media, including woven and nonwoven filters in the form of round tubes, are utilized in industrial processes [4]. These filters are favored for their affordability, ease of operation, and high efficiency in particle collection [5]. Filter bags, made from different materials and manufacturing processes, are employed in diverse working environments. The accumulation of particulate matter

within the fibrous filter affects pressure drop across three stages: depth filtration, transition, and surface filtration [6]. The depth filtration stage represents the clean, initial phase of the dust collection process, during which pressure drop increases linearly with airflow rate. At the end of this stage, the pressure drop begins to rise at a slightly faster rate. As dust continues to accumulate, the fabric becomes inefficient at filtration, and dust particles begin to collect on the surface, forming a dust cake. This shifts the pressure drop curve, which gradually increases [7]. Filter performance and pressure drop are closely interconnected; maintaining a balance between high filtration efficiency and manageable pressure drop is essential for cost-effective operation. A higher pressure drop indicates greater airflow resistance, serving as a key measure of operational resistance and air volume in dust collectors, while the outlet dust emission concentration is a critical indicator of dust removal efficiency. The required pressure drop is commonly used to determine the maximum filtration capacity, as higher filtration efficiency, which captures more particles, corresponds with a higher pressure drop [8, 9].

Filter performance is influenced by several factors, including the physical properties of the filter media (such as thickness, density, and air permeability), operating conditions (including airflow rate and fine particle properties), and the geometry of the bag filter (e.g., flat and pleated cylindrical cartridge filters). Various researchers have designed and conducted experiments to investigate the filtration performance of bag filters. For instance, the effect of airflow rate on bag filter efficiency was examined in a pilot-scale system with different can velocities. The experimental results demonstrated that inadequate operational speeds led to an inappropriate increase in the cleaning period, which in turn raised energy consumption and shortened the filter's service life. As a result, it was recommended that an appropriate can velocity be selected for real-scale equipment by testing on a pilot-scale bag filter dust collector [10]. Nonwoven fibrous materials offer several advantages, such as high porosity, complex structures, and varied pore size distribution. To enhance the filtration performance of nonwoven bag filters, the surface of the filter media was modified through surface finishing, which improved dust cake removal. The application of surface finishes increased the overall specific filtration resistance by 1.2 times for surface-finished filters and 4.2 times for membrane-finished filters compared to unfinished filters [11]. Baghouse development typically focuses on cylindrical filter bags, but flat cartridge filters can be pleated to expand the filtration area and reduce installation space. An increased filtration area lowers filtration velocity under the same air volume, thereby enhancing dust collection capacity. However, fine particles accumulate on the filter media over time, leading to a gradual rise in pressure drop, necessitating regular changes, increased energy consumption, and a shorter service life [12]. Teng et al. [13] sought to optimize the geometry of pleated filter bags and experimentally measured their effective filtration area. They found that when the pleat ratio (the ratio of pleat height to pleat pitch) ranged between 2.22 and 3.70, the effective filtration area increased with the pleat ratio. Overall, prior research indicates that filter performance is significantly affected by material properties, operating conditions, and filter geometry, often reflected in the pressure drop.

2. RESEARCH SIGNIFICANCE

This study addresses the overlooked physical properties of nonwoven filter media during initial air filtration. Using a pilot-scale baghouse with a flat cartridge filter, filtration performance was evaluated at airflow velocities of 0.5–3.0 m/s. Analysis of five materials with varying air permeability highlights their influence on filtration efficiency and pressure drop, stressing the need for strategic filter selection and maintenance. A second-order polynomial equation, aligned with the Darcy-Forchheimer model, was developed to predict pressure drop. The findings offer a robust framework for optimizing baghouse filtration systems, enhancing energy efficiency and operational performance while addressing a critical gap in industrial filtration research.

3. MATERIALS AND METHODS

Nonwoven fabrics are classified as porous media, making the theories related to flow through porous media applicable. Two primary theories govern this flow: the channel theory and the cell model theory. Channel theory, often exemplified by the capillary tube model, posits that the media consists of a bundle of cylindrical tubes that extend from one surface to another without requiring the flow to be perpendicular to the surfaces. Conversely, the cell model theory is associated with the drag model theory, which provides a different perspective on flow dynamics within the porous structure [14].

3.1 Flow Models

In this study, the Navier-Stokes equation governs fluid flow through porous media, including bag filters. This equation comprises the continuity and transient momentum equations, which are represented as follows [15–25]:

$$\frac{\partial}{\partial x_i}(\rho u_i) = 0 \quad (1)$$

$$\frac{\partial}{\partial t}(\rho u_i) + u_i \frac{\partial}{\partial x_i}(\rho u_i) = -\frac{\partial p}{\partial x_i} + \mu \frac{\partial \tau_{ij}}{\partial x_i} + S \quad (2)$$

$$S = -\frac{\Delta p}{L} \quad (3)$$

where ρ denotes the density, t denotes the time variation, u denotes the velocity vector, μ denotes the fluid viscosity, p denotes the pressure, τ denotes the shear stress tensor, S denotes a source term vector, Δp denotes the pressure drop, and L denotes the fabric filter thickness.

3.2 Porous Media Models

In porous media, the fluid permeation through a filter can be described by Darcy's law, which establishes the relationship between the average velocity and the pressure drop across the porous medium. Proposed by Henry Darcy, this law is based on experimental results of water flow through a filter bed. It states that the flow rate is directly proportional to the cross-sectional area of the sand and the difference in fluid head height between the inlet and outlet of the sand bed while being inversely proportional to the bed's thickness [26]. For a homogeneous and isotropic porous medium, Darcy's Law is expressed as [3]:

$$\Delta p = -\frac{\mu L}{K} u_i \quad (4)$$

where Δp denotes the pressure drop across the porous media (Pa), μ denotes the dynamic viscosity of the fluid (Pa.s), u denotes the velocity of the fluid through the porous media, and L and K denote the thickness (m) and the permeability of the porous media, respectively.

The Darcy-Forchheimer equation extends Darcy's law by accounting for both viscous and inertial effects in porous media. Filters with dense structures frequently encounter these effects, making the Darcy-Forchheimer equation essential for accurately modeling fluid flow through such media. This equation is particularly valuable in situations where both viscous and inertial forces contribute significantly to the pressure drop. It describes the pressure drop due to friction within the porous medium as a function of the flow velocity through the material [3, 27], and is expressed as follows:

$$\Delta p = \mu L D u_i + \frac{\rho L}{2} F {u_i}^2 \quad (5)$$

where D denotes the linear resistance coefficient and F denotes the quadratic resistance coefficient.

3.3 Filter Samples

In this study, nonwoven fabrics, which are typically simple random fiber structures in sheet form, are employed to separate different phases from the fluid passing through the bag filter media. Table 1 outlines the specifications of each nonwoven fabric, determined through standardized testing and provided by the manufacturers. All filter media were obtained from Dust Control Co., Ltd. (Phasi Charoen, Bangkok, Thailand), a leading baghouse filter manufacturer that provided financial support for this study, specifically for use in bag filters. In the context of bag filters, the web and scrim refer to components of the filter media that enhance both structural strength and filtration efficiency. The integration of these elements results in a filter medium that optimally balances mechanical strength and filtration performance. The four types of filtration media utilized were Polytetrafluoroethylene (PTFE), Polyester (PE), M-Aramide, and Polyphenylene Sulphide (PPS), each possessing a distinct composition that led to unique structural differences. These nonwoven fabrics, with air permeability ranging from 49 to 300 mm/s at a standard testing pressure of 200 Pa, were used to construct the bag filters. Air permeability was measured according to EN ISO 9237-1995 standards, with calculations based on Eq. (6). Several samples of the bag filters were analyzed using scanning electron microscopy (SEM, Philips model: XL 30), with a resolution of 2 nm at 30 kV and 5 nm at 1 kV, under variable tension from 0.2 to 30 kV. Figure 1 presents SEM images of all filter media at 10 kV, revealing the membrane distribution and fibrous structure of the bag filters. The images, captured at a scale of 500 micrometers, provide a detailed view of the oriented filaments. The fiber diameters were not uniform across the samples, with the smallest fiber diameter observed in the lowest K, A-type filter. The average fiber diameters for A, B, C, D, and E-type filters were 0.30, 15.18, 20.80, 22.92, and 19.26 μm, respectively.

Table 1. Filter fabric specification from the manufacturer

Table 1 Specifications of filter fabrics provided by the manufacturer.

Type	Composition (web/scrim)	Area weight (g/m^2)	L (mm)	ρ (g/cm^3)	K (mm/s at 200 Pa)
A	PTFE/PTFE*	800	1.1	0.73	49
B	PE/PE**	650	2.2	0.33	117
C	PPS/PPS***	550	1.7	0.32	183
D	M-Aramide/ M-Aramide	550	2.3	0.24	250
E	PE/PE	500	1.3	0.31	300

*Note: *PTFE = Polytetrafluoroethylene, **PE = Polyester and ***PPS = Polyphenylene Sulphide.*

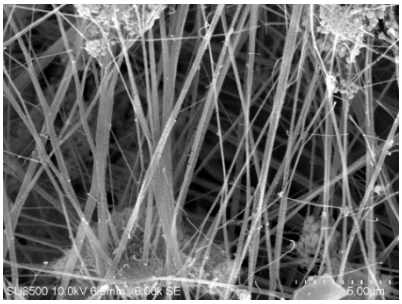

(a)

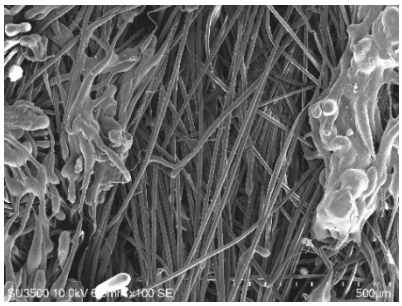

(b)

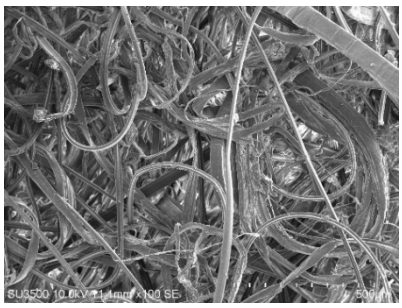

(c)

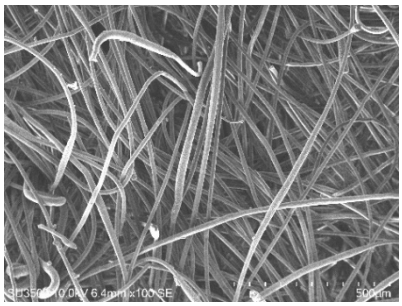

(d)

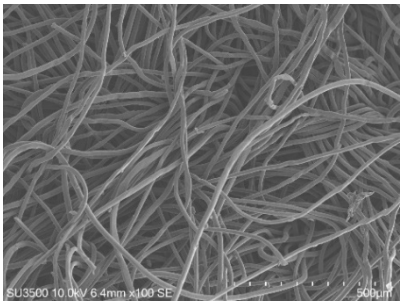

(e)

Fig. 1 SEM images of filters classified as: (a) A-type, (b) B-type, (c) C-type, (d) D-type, and (e) E-type, displayed at a scale of 1:500 µm.

$$K = \bar{q}_{\forall}/_{A} \quad (6)$$

where K denotes the air permeability, $\bar{q}_{\forall}$ denotes the arithmetic mean flow rate of air, and A denotes an area of fabric under test in square millimeters.

3.4 Bag Filter Testing

Laboratory tests were conducted on a pilot-scale dust collector equipped with a single cylindrical cartridge bag filter positioned at the center of the test unit to evaluate the filtration performance at the initial stage of filtration [3]. The baghouse design, illustrated in millimeter units in Fig. 2, had a total height of 2,450 mm and was divided into two chambers: the top chamber (450 mm in height) and the housing chamber (1,100 mm in height), separated by a square plate with a central hole for installing the cartridge filter. Both chambers had a cross-sectional area of 750×750 mm². The hopper wall, attached to the air inlet, had its cross-sectional area reduced from 750×750 mm² to 250×250 mm² over a height of 450 mm. Five types of nonwoven bag filters, each with a height of 1,000 mm and a diameter of 150 mm, were used in this study. The fabricated baghouse is shown in Fig. 3. The test was conducted using clean air at a room temperature of 25 °C and a relative humidity of 60%, propelled by a blower to maintain a constant volumetric flow rate. The baghouse was equipped with a single radial through the outlet. The average velocity varied between 0.5 and 3.0 m/s, in increments of 0.5 m/s. A blower inverter, adjustable within a frequency range of 10 to 50 Hz, was used to regulate the filtration velocities. nonwoven filter cartridge, allowing for a focused investigation of the nonwoven media's effect on pressure drop and filtration velocity. To eliminate the influence of filter shape on these parameters, all nonwoven media were configured into cylindrical cartridges, ensuring

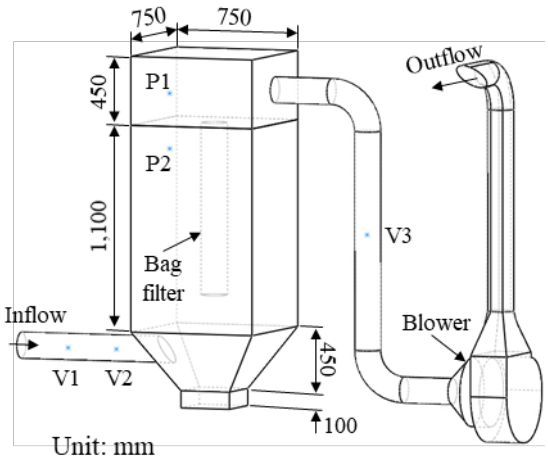

Fig. 2 Schematic diagram of the pilot-scale filter unit, illustrating the inlet pipe, baghouse with a bag filter, outlet pipe, and blower.

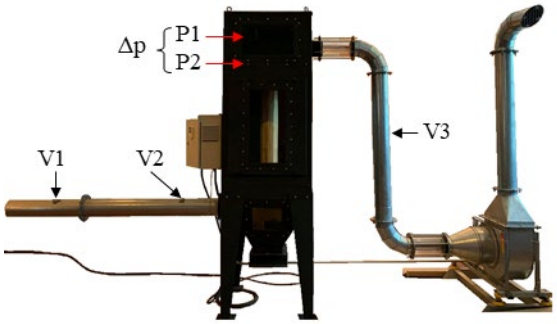

Fig. 3 Pilot-scale baghouse filter system.

that variations in filtration performance could be attributed solely to the properties of the nonwoven materials rather than differences in filter geometry.

The air velocity was measured using a pressure and flow meter (DT-8920, CEM). The inlet airflow velocity is recorded at points V1 and V2, located in the middle of the inlet duct, to capture the air inlet velocity (Fig. 4). The exhausted airflow was measured at point V3 on the exhaust duct to determine the air outlet velocity (Fig. 5). Point V2

Fig. 4 Measurement of the inlet air velocity at location V2.

Fig. 5 Measurement of the exhaust air velocity at location V3.

Fig. 6 Measurement of the pressure drop within the baghouse.

was positioned 400 mm horizontally from the baghouse wall, and the distance between V1 and V2 was 1,100 mm. Point V3, on the exhaust duct, was located 650 mm vertically from the air outlet. The pressure drop inside the baghouse is measured between the housing and top chambers using the same pressure and flow meter, which had an accuracy of ±2.5% for velocity and ±0.3% for pressure measurements (Fig. 6). Each experiment was repeated five times at each outlet velocity, and all tests were conducted under air-conditioned conditions, maintaining an ambient temperature of 25°C.

4. RESULTS AND DISCUSSION

This section presents and discusses the results of tests conducted on cylinder filter bags made from various nonwoven media within a lab-scale baghouse filter, all under identical experimental conditions. Furthermore, the pressure drop characteristics observed for each cylinder filter were utilized to develop a mathematical model, facilitating a deeper understanding of the filtration dynamics.

4.1 Evaluation of Bag Filter Performance

In the performed experiments, the pilot-scale baghouse filter varied the outlet velocity from 0.5 to 3.0 m/s in 0.5 m/s increments and measured inlet and outlet velocities and pressure drop. Fig. 7 shows the variation in the pressure drop acquired by five filter media with various filtration velocities, which had been maintained in a clean condition. This figure depicting the relationship between pressure drop and filtration velocity was essential for comprehending the performance characteristics of a filter medium to capture dust particles of different sizes. As expected, the pressure drop was almost linear with the increased filtration velocity. For a given filtration velocity, the inlet flow rate is directly proportional to the air permeability of the filter media. As a result, an

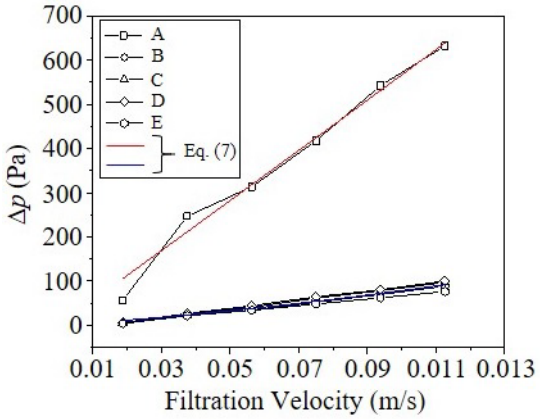

Fig. 7 Characteristics of the baghouse filter utilizing filter bags with varying air permeabilities.

increase in the inlet flow rate leads to a higher pressure drop. This finding is consistent with prior research [3, 6]. To maintain the specific filtration velocity, higher pressure drops lead to increased energy consumption for the fans that drive the fluid through the filter. Notably, these results align closely with the pressure drop values of clean filter media reported in the experiment by Jin et al. [28], although the air permeability of the filter bags in their study remained constant throughout the investigation.

The linearity between filtration velocity and pressure drop can be categorized into two distinct groups: one demonstrating the highest pressure drop and the other exhibiting similar characteristics. The A-type filter demonstrates the highest pressure drop due to its lowest air permeability of 49 mm/s, which was linked to the porous structure of the fabric. Scanning electron microscopy (SEM) results indicate that the A-type filter has the smallest fiber diameter at 0.30 μm, along with the highest packing density and area weight. Both fiber diameter and packing density significantly influence pressure drop; thinner fibers create smaller pores, resulting in more complex airflow pathways that increase pressure drop. Conversely, the pressure drop across the other filters is notably lower than that of the A-type filter at all comparable flow rates. These other filter bags exhibit similar characteristics in fiber diameter, packing density, and area weight, with values ranging from 15.18 to 22.92 μm, 0.24 to 0.33 g/cm³, and 500 to 650 g/m², respectively, and air permeability between 117 and 300 mm/s. Consequently, it can be concluded that this group of filter bags, with material properties within these ranges, does not exhibit significant differences in filtration resistance. However, a packing density exceeding twice that of this group resulted in a high-pressure drop and an A-type sharp deviation. During the initial filtration stage, the pressure drop is typically low because the filter media is clean and the airflow path is unobstructed. A higher initial pressure drop indicates an enhanced capability to trap smaller dust particles. As the filtration system operates, dust particles accumulate in the filter media, increasing flow resistance and consequently raising the pressure drop. This increase is influenced by the type of dust particles, flow rate, and filter media properties. When the pressure drop reaches a critical level, the system may require maintenance. Thus, the filter's lifespan is directly related to both the rate of increase in pressure drop and its initial value. Selecting the appropriate filter bag is crucial for ensuring effective operation before maintenance, cleaning, or replacement of the filter media is necessary, which can ultimately reduce operational costs.

4.2 Pressure Drop Modeling

A model for pressure drop can be generated using Equation (5), which incorporates two coefficients, D and F. To estimate these coefficients within the context of the Darcy-Forchheimer equation, experimental data were analyzed to establish the relationship between pressure drop and filtration velocity. A nonlinear regression method was utilized to fit the experimental data to a second-order polynomial equation, as shown in Equation (7). The coefficients D and F can be derived by comparing the polynomial coefficients from Equation (5) and Equation (7), as shown in Equations (8) and (9), respectively.

$$\Delta p = a u_i + b u_i^2 \quad (7)$$

$$D = a/\mu L \quad (8)$$

$$F = 2b/\rho L \quad (9)$$

where Δp denotes pressure drop, u_i denotes the filtration velocity, D denotes the linear resistance coefficient, μ denotes the dynamic viscosity of the fluid, F denotes the quadratic resistance coefficient, ρ denotes the fluid density, L denotes the fabric filter thickness, and a and b denote a constant of a pressure drop model.

In this analysis, the dynamic viscosity (μ) and density (ρ) of air were measured at values of 1.86×10^{-5} Pa·s and 1.16 kg/m³, respectively. Consequently, the nonlinear regression analysis of the experimental data using Equation (7) demonstrated high accuracy, yielding an R^2 value of 0.989 for A-type filters and values ranging from 0.992 to 0.995 for B- to E-type nonwoven filters. The resulting two coefficients are presented in Table 2. Equation (7) effectively predicts pressure drop by incorporating both viscous and inertial contributions. To manage experimental uncertainties, rigorous instrument calibration was conducted, alongside repeated experiments to ensure statistical validity. Controlled environmental conditions were maintained, and data averaging was employed to mitigate anomalies.

Table 2 Coefficients of the pressure drop model.

Type	*a*	*b*	R^2
A	5,624.71	424.34	0.989
B	539.26	2,473.90	0.995
C	539.26	2,473.90	0.994
D	539.26	2,473.90	0.993
E	539.26	2,473.90	0.992

Additionally, a detailed error analysis and cross-validation with theoretical predictions were performed. These procedures ensure the robustness of the results, facilitating improved filter design and performance predictions in baghouse filter systems.

5. CONCLUSION

Baghouse filters are extensively employed in various applications for air pollution control by effectively capturing fine dust particles. Understanding the performance of filter media in relation to pressure drop is crucial for ensuring efficient operation, thereby facilitating the selection of the appropriate filter bag based on specific needs. This study utilized a pilot-scale baghouse filter to investigate the performance of five different filter media under clean conditions. The main findings and conclusions of this study are outlined below:

1) A pilot-scale baghouse equipped with a single cartridge nonwoven bag filter was constructed to assess the performance of the five filter media. The properties of the nonwoven fabrics were determined through standard testing in accordance with EN ISO 9237:1995 and scanning electron microscopy (SEM) methods. The experimental pressure drop data correlated well with the material properties, including air permeability, packing density, and fiber diameter.

2) The pressure drop across the baghouse filter for each filter cartridge with different nonwoven media exhibited a linear relationship with respect to the filtration velocities. However, the curve fitting using a polynomial equation provided the best accuracy. Consequently, the pressure drop models are represented as polynomial functions.

3) The pressure drop across the bag filter increased with an increase in filtration velocity. At comparable filtration velocities, the pressure drop values could be categorized into two groups: higher and similar values. The higher pressure drop was associated with the A-type filter bag, which exhibited the lowest air permeability, smallest fiber diameter, and highest packing density.

4) The Darcy-Forchheimer equation for porous media was employed to fit the two groups of pressure drops. These equations accurately predict pressure drop by accounting for both viscous and inertial contributions.

5) Operating a baghouse filter at velocities where the pressure drop increases significantly can lead to inefficiencies and higher operational costs. The developed models assist in designing efficient filtration systems by balancing filtration efficiency and pressure drop, ensuring optimal operation within the desired velocity range for effective dust particle capture.

However, a primary limitation of using the Darcy-Forchheimer equation for porous media in this study is its limited applicability to the jet pulse cleaning time for accumulated dust on the filter. To address this, the baghouse will be enhanced to facilitate experiments involving accumulated dust. This challenge will be tackled in future research.

6. ACKNOWLEDGMENTS

This research was financially supported by the Thailand Research Fund (TRF) and Dust Control Co., Ltd., under TRF Research Grant No. MSD62I0010.

7. REFERENCES

[1] Waluś K.J., Warguła Ł., Krawiec P., Adamiec J. M., Legal regulations of restrictions of air pollution made by non-road mobile machinery—the case study for Europe: a review, Environ. Sci. Pollut. R., Vol. 25, Issue 4, 2018, pp. 3243-3259.

[2] Bächler P., Meyer J., Ligotski R., Krug P., Dittler A., Measurement of transient nanoparticle emissions of a municipal biomass incineration plant equipped with pulse-jet cleaned filters, Process Saf. Environ. Prot., Vol. 184, 2024, pp. 601-614.

[3] Punyaponchai A., Priyadumkol J., Loksupapaiboon K., Thongkom S., Suvanjumrat C., Development of a baghouse filter CFD model for efficient particulate removal in air filtration systems, International Journal of GEOMATE, Vol. 26, Issue 113, 2024, pp. 82-89.

[4] Tian F., Jiang G., Gao Z., Preparation and filtration performance of the circular weft-knitted seamless weft-insertion fabric materials, J. Ind. Text., Vol. 50, Issue 8, 2021, pp. 1145-1164.

[5] Ali, S.B., Ghasemi H., Ahmadi R., Ghaffari A., Recent progresses in dry gas polymeric filters. Energy Chem., Vol. 62, 2021, pp. 103-119.

[6] Teng, G., Shi G., Zhu J., Influence of pleated geometry on the pressure drop of filters during dust loading process: experimental and modelling study, Sci. Rep., Vol. 12, Issue 1, 2022, pp. 20331.

[7] Zhang, F., Ding Y., Low Z.X., Jia L., Zhou G., Liu Y., Zhong Z., Xing W., Effects of flow distributor structures and particle-wall

interaction on baghouse gas-solid flow, Sep. Purif. Technol., Vol. 335, 2024, pp. 126140.

[8] Li, J., Chen D.R., Li S., Zhou F., Reverse pulsed-flow cleaning for filtration unit regeneration: A review, Sep. Purif. Technol., Vol. 330, 2024, pp. 125441.

[9] Li S., Wang L., Wen G., Jin H., Cheng H., Liu L., Yuan L., Zhou F., Influence of air inlet and cleaning chamber on the performance of mining cartridge filter, Adv. Powder Technol., Vol. 33, Issue 11, 2022, pp. 103796.

[10] Joe Y. H., Shim J., Park H.S.., Evaluation of the can velocity effect on a bag filter, Powder Technol., Vol. 321, 2017, pp. 454-457.

[11] Fukasawa T., Kanaoka C., Ishigami T., Fukui K., Effects of surface finish of nonwoven fabric bag filters on filter efficiency, Chem. Eng. Technol., Vol 45, 2022, pp. 92-99.

[12] Kim J.S., Lee M.H., Measurement of effective filtration area of pleated bag filter for pulse-jet cleaning, Powder Technol., Vol. 343, 2019, pp. 662-670.

[13] Teng, G., Shi G., Zhu J., Qi J., Zhao C., Research on the influence of pleat structure on effective filtration area during dust loading, Powder Technol., Vol. 395, 2022, pp. 207-217

[14] Sambaer W, Zatloukal M., Kimmer D., 3D air filtration modeling for nanofiber based filters in the ultrafine particle size rang, Chem. Eng. Sci., Vol. 82, 2012, pp. 299-311.

[15] Domaingo D., Langmayr D., Somogyi B., Almbauer R., A semi-implicit treatment of porous media in steady-state CFD, Transp. Porous Med.,Vol. 112, 2016, pp. 451-466.

[16] Loksupapaiboon K., Suvanjumrat C., Curing analysis of rubber film on a hand-shaped former in the manufacturing of rubber gloves through novel OpenFOAM solver, International Journal of Heat and Fluid Flow, Vol. 108, 2024, pp. 109476. https://doi.org/10.1016/j.ijheatfluidflow.2024.109476

[17] Kamma P., Promtong M., Suvanjumrat C., Development of a reduced mechanism for methane combustion in Open FOAM: A computational approach for efficient and accurate simulations, International Journal of Thermofluids, Vol. 22, 2024, pp. 100654. https://doi.org/10.1016/j.ijft.2024.100654

[18] Loksupapaiboon K., Suvanjumrat C., Forced convective heat transfer and fluid flow past a rotating hand-shaped former for improving rubber glove curing, Case Studies in Thermal Engineering, Vol. 47, 2023, pp. 103050. https://doi.org/10.1016/j.csite.2023.103050

[19] Kamma P., Suvanjumrat C., A novel diffusion flux modeling for laminar premixed flame simulation with OpenFOAM, Results in Engineering, Vol. 20, 2023, pp. 101462. https://doi.org/10.1016/j.rineng.2023.101462

[20] Loksupapaiboon K., Suvanjumrat C., Experiment and numerical Studies of convection heat transfer around a rotating hand-shaped former, Heat Transfer Engineering, Vol. 45, Issue 22, 2024, pp. 2006–2028.

[21] Loksupapaiboon K., Suvanjumrat C., Effects of flow and heat transfer around a hand-shaped former, Engineering Applications of Computational Fluid Mechanics, Vol. 16, Issue 1, 2022, pp. 1619-1640.

[22] Suvanjumrat C., Loksupapaiboon K., Development of cure kinetics models for drying nitrile-butadiene rubber latex film with computational fluid dynamics simulation, International Journal of Thermofluids, Vol. 25, 2025, pp. 101022. https://doi.org/10.1016/j.ijft.2024.101022

[23] Kamma P., Suvanjumrat C., Assessment of partially premixed flame by in-situ adaptive reduced mechanisms in OpenFOAM, International Journal of Automotive and Mechanical Engineering, Vol. 18, Issue 4, 2021, pp. 9220-9229.

[24] Suvanjumrat C., Loksupapaiboon K., Improvement of thermal distribution in the rubber-glove former conveyor oven by OpenFOAM, Engineering Journal, Vol. 24, Issue 2, 2020, pp. 109-120.

[25] Chaichanasiri E, Suvanjumrat C., Simulation of three dimensional liquid-sloshing models using C++ open source code CFD software, Kasetsart J. (Nat. Sci.), Vol. 46, 2012, pp. 978-995.

[26] Simmons C. T., Henry Darcy (1803-1858): Immortalised by his scientific legacy, Hydrogeol. J., Vol. 16, 2007, pp. 1023-1038.

[27] Ehlers W., Darcy, Forchheimer, Brinkman and Richards: classical hydromechanical equations and their significance in the light of the TPM, Arch. Appl. Mech., Vol.92, 2022, pp. 619–639.

[28] Jin H., Li S., He S., Hu S., Yuan L., Zhou F., The pressure drop of fibrous surface filters for gas filtration: modeling and experimental studies, Separation and Purification Technology, Vol. 350, 2024, pp. 127961.